Liquid–liquid phase separation and morphologies in organic particles consisting of α-pinene and β-caryophyllene ozonolysis products and mixtures with commercially-available organic compounds

Young-Chul Song[1], Ariana G. Bé[2], Scot T. Martin[3], Franz M. Geiger[2], Allan K. Bertram[4], Regan J. Thomson[2], and Mijung Song[1*]

[1]Department of Earth and Environmental Sciences, Jeonbuk National University, Jeollabuk-do, Republic of Korea

[2]Department of Chemistry, Northwestern University, Evanston, Illinois 60208, United States

[3]School of Engineering and Applied Sciences & Department of Earth and Planetary Sciences, Harvard University, Cambridge, Massachusetts 02138, United States

[4]Department of Chemistry, University of British Columbia, Vancouver, BC, V6T 1Z1, Canada

Correspondence: Mijung Song (mijung.song@jbnu.ac.kr)

Abstract

Liquid–liquid phase separation (LLPS) in organic aerosol particles can impact several properties of atmospheric particulate matter, such as cloud condensation nuclei (CCN) properties, optical properties, and gas-to-particle partitioning. Yet, our understanding of LLPS in organic aerosols is far from complete. Here, we report on LLPS of one-component and two-component organic particles consisting of α-pinene- and β-caryophyllene-derived ozonolysis products and commercially-available organic compounds of relevance to atmospheric organic particles. In the experiments involving single-component organic particles, LLPS was observed in 8 out of 11 particle types studied. LLPS almost always occurred when the oxygen-to-carbon elemental ratio (O:C) was ≤ 0.44, but did not occur when O:C was > 0.44. The phase separation occurred by spinodal decomposition and nucleation and growth mechanism, and when LLPS occurred, two liquid phases co-existed up to ~100% relative humidity (RH). In the experiments

involving two-component organic particles, LLPS was observed in 23 out of 25 particles types studied. LLPS almost always occurred when the average was O:C ≤ 0.67, but never occurred when the average O:C was > 0.67. The phase separation occurred by spinodal decomposition and nucleation and growth mechanisms. When LLPS occurred, two liquid phases co-existed up to ~100%. These results provide further evidence that LLPS is likely a frequent occurrence in organic aerosol particles in the troposphere, even in the absence of inorganic salts.

1. Introduction

Secondary organic aerosols (SOA) are ubiquitous in the atmosphere, comprising up to approximately 80% of the mass of submicrometer particles (Kanakidou et al., 2005; Jimenez et al., 2009; Heald et al., 2010). SOA particles are produced when OH, NO_3, and O_3 oxidize volatile organic compounds (VOC) in the atmosphere. Depending on the VOC type, oxidant type, and reaction time, the oxygen-to-carbon elemental ratio (O:C) of SOA can vary from 0.2 to 1.0 (Zhang et al., 2007; Hallquist et al., 2009; Jimenez et al., 2009; Heald et al., 2010; Ng et al., 2010). SOA particles are important because they play critical roles in air quality, cloud formation, and the Earth's radiative properties (Seaton et al., 1995; Xiaohong and Jian, 2010; Pöschl and Shiraiwa, 2015; Sanchez et al., 2017; Shiraiwa et al., 2017).

SOA can undergo phase transitions as relative humidity (RH) changes in the atmosphere (Hänel, 1976; Martin, 2000; Krieger et al., 2012; You et al., 2014; Freedman, 2017). One possible phase transition is liquid–liquid phase separation (LLPS) (Pankow, 2003; Marcolli and Krieger, 2006; Ciobanu et al., 2009; Bertram et al., 2011; Krieger et al., 2012; Song et al., 2012a; Zuend and Seinfeld, 2012; Veghte et al., 2014; You et al., 2014; Obrien et al., 2015; Freedman, 2017; Zhang et al., 2018, 2019; Olson et al.,2019; Riva et al., 2019). The occurrence of LLPS has implications for the optical properties (Brunamonti et al., 2015; Fard et al., 2018), gas-particle partitioning (Zuend et al., 2010; Zuend and Seinfeld, 2012; Shiraiwa et al., 2013), hygroscopic properties (Hodas et al., 2016), and cloud condensation nuclei (CCN) properties (Ovadnevaite et al., 2017; Liu et al. 2018) of atmospheric particles.

Many researchers have focused on LLPS in particles containing organic material mixed with inorganic salts. They found that LLPS can occur when the O:C of the organic material is smaller than 0.8 (Bertram et al., 2011; Krieger et al., 2012; Song et al., 2012a, 2012b; Schill and Tolbert, 2013; You et al., 2013,

2014). More recently, studies on LLPS in organic aerosol particles free of inorganic salts have shown that LLPS occurs in SOA generated in environmental chambers when the average O:C of the organic material is smaller than roughly 0.5 across the RH range of ~95% to ~100% (Renbaum-Wolff et al., 2016; Rastak et al., 2017; Song et al., 2017; Ham et al., 2019) with implications for the CCN properties of the SOA (Petters et al., 2006; Hodas et al., 2016; Renbaum-Wolff et al., 2016; Ovadnevaite et al., 2017; Rastak et al., 2017; Liu et al., 2018; Ham et al., 2019). In addition, Song et al. (2018) showed that LLPS occurs in organic particles containing one commercially-available organic compound when the O:C is smaller than 0.44 while LLPS occurs in organic particles containing two commerically available organic species when the average the O:C is smaller than ≤ 0.58.

In the following, we investigated LLPS in particles containing one and two organic species generated from ozonolysis products of α-pinene and β-caryophyllene, which are atmospherically relevant, and commercially-available organic compounds. α-pinene and β-caryophyllene are the most abundant types of monoterpene ($C_{10}H_{16}$) and sesquiterpenes ($C_{15}H_{24}$) in the atmosphere, respectively (Guenther, 1995; Sakulyanontvittaya et al., 2008; Henrot et al., 2017). However, the studies of LLPS and morphologies for α-pinene and β-caryophyllene oxidation products are still rare. Our results can provide additional insight into the O:C range required for LLPS in organic particles free of inorganic salts. Moreover, our results can provide that the chemical complexity of organic particles effects on LLPS. These observations should improve our understanding of LLPS behavior and provide more accurate constrained the value of the O:C ratio for LLPS. The results from these studies should also improve the understanding and modelling of CCN activity of SOA free of inorganic salts.

2. Experimental

2.1 Materials

Table 1 presents the physical properties of the organic compounds investigated. In this study, 11 organic species were used, including seven products from the ozonolysis of α-pinene and β-caryophyllene and four commercially-available organic compounds. These species covered an O:C range of 0.13 - 1.00 (Table 1). All species were liquid at room temperature.

Seven of the products from the ozonolysis of α-pinene and β-caryophyllene were synthesized. The detailed synthesis methods for these species are described in Bé et al. (2017). Using ^{1}H NMR, ^{13}C NMR, and IR spectroscopy, the ozonolysis products were characterized to confirm their identity and purity. The purity of all synthesized compounds was > 95%. All products contained a carboxylic acid, ketone, and/or aldehyde, which are abundant organic functional groups in the atmosphere (Hallquist et al., 2009; Nozière et al., 2015). The O:C range of the ozonolysis products was between 0.13 and 0.44 (Table 1). To achieve O:C ratios up to 1.00, we used commercially-available organic compounds (Sigma-Aldrich, purities ≥ 97%) (Table 1).

2.2 Preparation of particles consisting of one and two organic species

Particles consisting of either one or two organic compounds were prepared at room temperature without the addition of a solvent. Particles consisting of the commercially-available organic compounds were nebulized directly on siliconized hydrophobic glass slides (Hampton Research, Canada). Particles consisting of ozonolysis products were slightly viscous. To form particles on a substrate, these ozonolysis products were picked up with the tip of a pipette, and the pipette was then flicked towards a hydrophobic glass slide.

Particles consisting of two organic compounds were prepared using mixtures (1:1 mass ratio) of pure organic species without addition of a solvent. To prepare the mixtures with 1:1 mass ratio, each organic species was weighed in a vial and then combined. After mixing, the solutions were homogenous based on visual inspection. Particles were generated from these mixtures and deposited on hydrophobic slides either by nebulization (for the mixtures involving commercially-available organic compounds) or by the flicking method via the tip of a pipette as described above (for the ozonolysis products). This method of producing two-component organic particles did not work for α-pinene ozonolysis products and β-caryophyllinic acid due to the stickiness of these material. Hence, these materials were not included in the systems used to generate two-component organic particles.

2.3 Optical microscopy for observation of liquid–liquid phase separation

The organic particles on hydrophobic glass slides were placed into a RH and temperature controlled flow-cell coupled to an optical microscope (Olympus BX43, 40× objective, Japan) (Parsons et al., 2004; Pant et al., 2006; Bertram et al., 2011; Song et al., 2012a, 2018; Ham et al., 2019). During all experiments, the temperature inside the flow-cell was maintained at 291 ± 1 K. The RH was controlled by a continuous flow of a wet and dry N_2 mixture with a total flow rate of 500 sccm. The temperature and RH were monitored by a humidity and temperature sensor (Sensirion, SHT 71, Switzerland). RH inside the flow-cell was calibrated by measuring the deliquescence RH of four different pure inorganic salts (potassium carbonate, sodium chloride, ammonium sulfate, and potassium nitrate) (Winston and Bates, 1960). The RH uncertainty from the calibration was ±1.5%.

At the beginning of LLPS experiments, organic particles inside the flow-cell were equilibrated at ~100% RH for 15–20 min. If LLPS was observed, the RH was decreased from ~100% to ~5-10% lower than the RH at which the two liquid phases merged into one phase followed by an increase in RH to ~100%. If LLPS was not observed, the RH was decreased from ~100% to ~0% RH, followed by an increase to ~100% RH. During all experiments, the RH was adjusted at a rate of $0.1 – 0.2\%$ RH min^{-1}. The optical images during experiments were recorded every 5 s using a CMOS (complementary metal–oxide–semiconductor) detector (DigiRetina 16, Tucsen, China). Organic particles were selected in the diameter range of 30–100 µm, which was required for LLPS experiments. Each one and two organic species was measured 4-5 times within this size range.

3. Results and discussion

3.1 Liquid–liquid phase separation in particles containing one organic species

Eleven different types of particles containing one organic species were investigated for LLPS at 291 ± 1 K. Out of the eleven different types of one-component organic particles studied, eight underwent LLPS during humidity cycles (Table S1). LLPS occurred in all one-component organic particles containing α-pinene and β-caryophyllene ozonolysis products.

Shown in Figure 1 and Movies S1-S7 are optical images recorded while the RH was decreased for all the cases where LLPS was observed in one-component organic particles. For these cases, two liquid phases were always observed at ~100% RH. As the RH was decreased, the two liquid phases merged into

one liquid phase at ~95% RH, except for particles of β-caryophyllinic acid (Fig. 1e and Movie S5). For β-caryophyllinic acid particles, the two liquid phases merged into one liquid phase at 82.1% RH (Fig. 1e and Movie S5).

Shown in Figure 2 and Movies S8-S14 are optical images of the same seven particles shown in Fig. 1 and Movies S1-S7, except the images were recorded while the RH was increased, rather than decreased. At low RH-values, the particles contained one phase. As the RH increased, LLPS occurred at ~95% RH for all cases exception for β-caryophyllinic acid particles, which underwent LLPS at 82.9% RH (Fig. 2e and Movie S12). At the onset of LLPS, many small inclusions formed in the particles. As the RH was further increased, the small inclusions coagulated and coalesced, and the particles continued to grow (Fig. 2 and Movies S8-S14). At ~100% RH, all particles contained two liquid phases. These results for LLPS occurrence in the organic particles was consistent within the studied size ranges (~30-100 µm in diameter).

LLPS in the single component organic particles occurred by nucleation and growth, and spinodal decomposition with RH increasing. Particles of β-nocaryophyllonic acid and suberic acid monomethyl ester (Song et al. 2018) had two liquid phases with inclusions by nucleation and growth mechanism (Fig. 2d and Movies S11) while the other single component organic particles had a core-shell morphology by spinodal decomposition (Fig. 2a, b, c, e, f, g and Movies S8, 9, 10, 12, 13, 14). Nucleation and growth mechanism is a phase transition which has to be overcome an energy barrier to form stable nuclei of the second phase within a liquid (Shelby, 1995; Papon et al., 1999; Ciobanu et al., 2009; Song et al., 2012a). Spinodal decomposition is a phase transition that occurs within a liquid without an energy barrier (Shelby, 1995; Papon et al., 1999; Ciobanu et al., 2009; Song et al., 2012a). Previous studies also observed LLPS by spinodal decomposition in α-pinene-derived SOA, β-caryophyllene-derived SOA, and limonene-derived SOA (Renbaum-Wolff et al., 2016; Song et al., 2017; Ham et al., 2019). We expect that the inner phase consisted mainly of water while the outer phase consisted mainly of organic molecules because the amount of the inner phase reduced in size as the RH was decreased (Renbaum-Wolff et al., 2016; Song et al., 2017, 2018). This assumption has also been reported in several other studies (Renbaum-Wolff et al., 2016; Song et al. 2017, 2018; Ham et al. 2019). The surface tension of water and the surface tensions of organics are consistent with this assumption (Jasper, 1972).

Illustrated in Fig. 3a is the lower RH boundary for LLPS (LLPS$_{lower}$) and upper RH boundary for LLPS (LLPS$_{upper}$) determined for one-component organic particles (blue symbols). LLPS occurred in the one-component organic particles when the O:C was $\leq$ 0.44. Our results are consistent with the results from Song et al. (2018), who observed LLPS in one-component organic particles when the O:C was $\leq$ 0.44 (Fig. 3a, grey symbols). Our results are also consistent with LLPS$_{lower}$ and LLPS$_{upper}$ determined for SOA produced from α-pinene and β-caryophyllene (Renbaum-Wolff et al., 2016; Song et al., 2017; Ham et al., 2019). In all cases, LLPS$_{upper}$ was ~ 100% RH.

The values of LLPS$_{lower}$ and LLPS$_{upper}$ determine in the current experiments using a decreasing RH was within the uncertainty of LLPS$_{lower}$ and LLPS$_{upper}$ values determine in the experiments using an increasing RH (Tables S1 and S2). In addition, no dependence on particle size was observed for LLPS$_{lower}$ and LLPS$_{upper}$ within the size range investigated (30–100 μm).

3.2 Liquid-liquid phase separation in particles containing two organic species

To better mimic the complexity of real aerosol compositions, we also studied LLPS in particles containing two organic species. Table S2 lists the 25 different mixtures investigated using combinations of β-caryophyllene ozonolysis products and commercially-available organic compounds. In total, 23 out of the 25 two-component organic particle types investigated underwent LLPS (Fig. 3b and Table S2). Shown in Fig. 4 and Movies S15-S19 are examples of images of two-component organic particles that underwent LLPS during a decrease in RH. Shown in Fig. 5 and Movies S20-S24 are the same five particles, but images recorded as the RH was increased.

Out of the 23 particles types that underwent LLPS, 22 of the particle types formed a core-shell morphology with decreasing RH. Only one particle type (β-caryophyllonic acid/β-nocaryophyllonic acid) was observed both core-shell and partially engulfed morphology with increasing RH (Fig. S1). As discussed in Sect. 3.1, the inner phase is expected to be mainly water while the outer phase is expected to be mainly organic material (Renbaum-Wolff et al., 2016; Song et al., 2017, 2018). As RH was decreased, the two liquid phases merged into one phase. For example, particles of β-caryophyllene aldehyde/PEG-400 merged into one phase at 39.9% RH (Fig. 4e and Movie S19).

Interestingly, particles showed different morphologies of core-shell, partially engulfed, and inclusions after LLPS occurred for RH increasing. These different morphologies have been also observed previously (Kwamena et al., 2010; Reid et al., 2011; Song et al., 2012a, 2013). The different morphologies could be resulted from the phase separation mechanisms, volume ratios and different functional groups (dicarboxylic acid vs carboxylic acid and ketone) which can result in different interfacial energies and spreading coefficients (Kwamena et al., 2010; Reid et al., 2011; Song et al., 2013; Stewart et al., 2015, Gorkowski et al. 2020).

In the experiments with two-component organic particles and increasing RH, in most cases (19 out of the 23 particle types that underwent LLPS), phase separation began with the abrupt formation of many small inclusions (e.g. Fig. 5a, b, e and Movies S20, 21, 24). This behavior suggests spinodal decomposition as the mechanism for LLPS. In contrast, the mechanism for LLPS in the particles containing ozonolysis products mixed with pyruvic acid was likely nucleation and growth mechanism based on the appearance of nucleation from the interior of the particles as the RH increased (Figs. 5c, d and Movies S22, 23).

Illustrated in Fig. 3b (blue symbols) is the lower RH boundary for LLPS (LLPS$_{lower}$) and upper RH boundary for LLPS (LLPS$_{upper}$) determined in the experiments with two-component organic particles. LLPS was observed in all cases when the average O:C $\leq$ 0.67. When LLPS was observe, LLPS$_{upper}$ was ~ 100% RH. These results are similar to previous results from Song et al. (2018) (gray symbols in Fig. 3b), even though they studied different types of two-component organic particles. Figure 3b also presents Sigmoid-Boltzmann fits of all data points from Song et al. (2018) and the current study to parameterize LLPS$_{lower}$ (solid line) and LLPS$_{upper}$ (dashed line) as a function of O:C. The parametrizations of Sigmoid-Boltzmann fits are given in the Supplement Information (Sect. S3).

4. Atmospheric implications

O:C of organic materials has been used to interpret and parameterize hygroscopicity (Jimenez et al., 2009), oxidation (Heald et al., 2010; Kroll et al., 2011), and mixing thermodynamics of organic aerosol particles (Donahue et al., 2011; Hodas et al., 2016). Previous studies have shown LLPS in mixed organic and inorganic aerosol particles often occurs for O:C < 0.8 (Bertram et al., 2011; Krieger et al., 2012; Song

et al., 2012a, 2012b; Schill and Tolbert, 2013; You et al., 2013, 2014). Even in the absence of inorganic salts, the occurrence of LLPS was dependent on the O:C of organic materials (Renbaum-Wolff et al., 2016; Song et al., 2017; Song et al., 2018; Ham et al., 2019). Our results show that as compositional complexity increased from one organic species to two organic species, LLPS occurred over a wider range of average O:C values of organic materials (increasing from 0.44 to 0.67) (Figs. 3a and b). Considering the chemical complexity and the O:C ratio of organic particles in the troposphere (0.20 < O:C < 1.00) (Zhang et al., 2007; Hallquist et al., 2009; Jimenez et al., 2009; Heald et al., 2010; Ng et al., 2010), our result provided additional evidence that LLPS is likely a common feature of organic aerosols free of inorganic salts. A caveat is that the mixing ratio of 1:1 for two organic species and the chemical complexity used in our experiments is rather simple compared to the chemical complexity found in the atmosphere (Zhang et al., 2007; Hallquist et al., 2009; Jimenez et al., 2009). Further studies are needed to confirm LLPS in organic aerosols comprising of more complex mixtures with different mixing ratios. In addition to the O:C ratio, the types of organic functional groups present in the molecules are also likely important for LLPS (Song et al., 2012b) because different functional groups lead to different strengths of intermolecular interactions with water. Further studies are needed to elucidate the effect of functional groups on the occurrence of LLPS in organic particles.

LLPS in aerosol particles has an impact on heterogeneous reactions (Folkers et al. 2003; Anttila et al. 2006; Cosman and Bertram, 2008; Cosman et al. 2008; McNeill et al., 2008; Lam et al., 2019) and CCN (Petters et al., 2006; Hodas et al., 2016; Renbaum-Wolff et al., 2016; Ovadnevaite et al., 2017; Rastak et al., 2017; Liu et al., 2018). The reactive uptake of gas-phase oxidants can differ depending on the number of phases present in the particles (Folkers et al. 2003; Anttila et al. 2006; Cosman and Bertram, 2008; Cosman et al. 2008; McNeill et al., 2008; Lam et al., 2019). For example, the effective OH uptake coefficient of 3-methylglutaric acid/ammonium sulfate particle decreased with a factor of ~2.4 than the particle of 3-methylglutaric acid (Lam et al., 2019).The occurrence of LLPS in organic aerosol particles at high RH, as observed in the current studies, is important since LLPS at high RH can lower the barrier to CCN activation by decreasing the surface tension of the particles (Ovadnevaite et al., 2017; Rastak et al., 2017; Liu et al., 2018). A decrease in surface tension and lowering of the barrier to CCN, can lead to

an increase in cloud droplets numbers in the atmosphere, with implications for modelling the indirect effect of aerosols on climate (Ovadnevaite et al., 2017; Rastak et al., 2017).

250
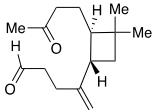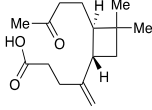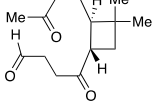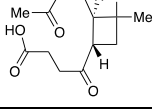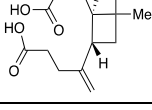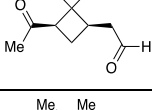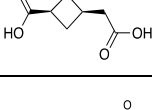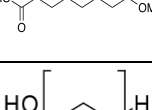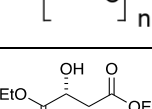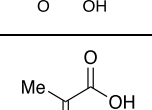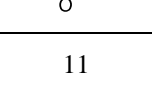
Data availability. Underlying material and related items for this paper are located in the Supplement.

Author contributions. MS, AKB, and RJT designed the study. YS and MS conducted LLPS experiments and analyzed the data. AGB, FMG, and RJT produced ozonolysis products. YS and MS prepared the
255   manuscript with contributions from AGB, STM, FMG, AKB, and RJT.

Competing interests. The authors declare that they have no conflict of interest.

Acknowledgements. For authors at Jeonbuk National University, this work was supported by the National
260   Research Foundation of Korea grant funded by the Korea Government (2019R1A2C1086187) and by Research Base Construction Fund Support Program funded from Jeonbuk National University in 2020. M. Song gives thanks to G. Jo for the technical support. The US National Science Foundation (AGS-1640378) is acknowledged by authors from Harvard University. The authors at Northwestern University acknowledge support from the US National Science Foundation (CHE-1607640 and Graduate Research
265   Fellowship to AGB).

Table 1. Molecular formula, molecular structure, molecular weight, oxygen-to-carbon elemental ratios (O:C), and functional groups of organic compounds studied. All compounds are liquid at room temperature.

Compounds		Molecular formula	Molecular structure	Molecular weight (g/mol)	O: C	Functional group
Ozonolysis products	β-caryophyllene aldehyde	$C_{15}H_{24}O_2$		237.19	0.13	Aldehyde, Ketone
	β-caryophyllonic acid	$C_{15}H_{24}O_3$		252.35	0.20	Carboxylic acid, Ketone
	β-nocaryophyllone aldehyde	$C_{14}H_{22}O_3$		238.32	0.21	Aldehyde, Ketone
	β-nocaryophyllonic acid	$C_{14}H_{22}O_4$		254.32	0.29	Carboxylic acid, Ketone
	β-caryophyllinic acid	$C_{14}H_{22}O_4$		254	0.29	Carboxylic acid
	Pinonaldehyde	$C_{10}H_{16}O_2$		169.12	0.20	Aldehyde, Ketone
	Pinic acid	$C_9H_{14}O_4$		209.08	0.44	Carboxylic acid, Ketone
Commercially-available organic compounds	Suberic acid monomethyl ester	$C_9H_{16}O_4$		188	0.44	Carboxylic acid, Ester
	Polyethylene glycol-400	$C_{2n}H_{4n+2}O_{n+1}$		400	0.56	Alcohol, Ether
	Diethyl L-tartrate	$C_8H_{14}O_6$		206	0.75	Alcohol, Ester
	Pyruvic acid	$C_3H_4O_3$		88.06	1.00	Carboxylic acid, Ketone

270
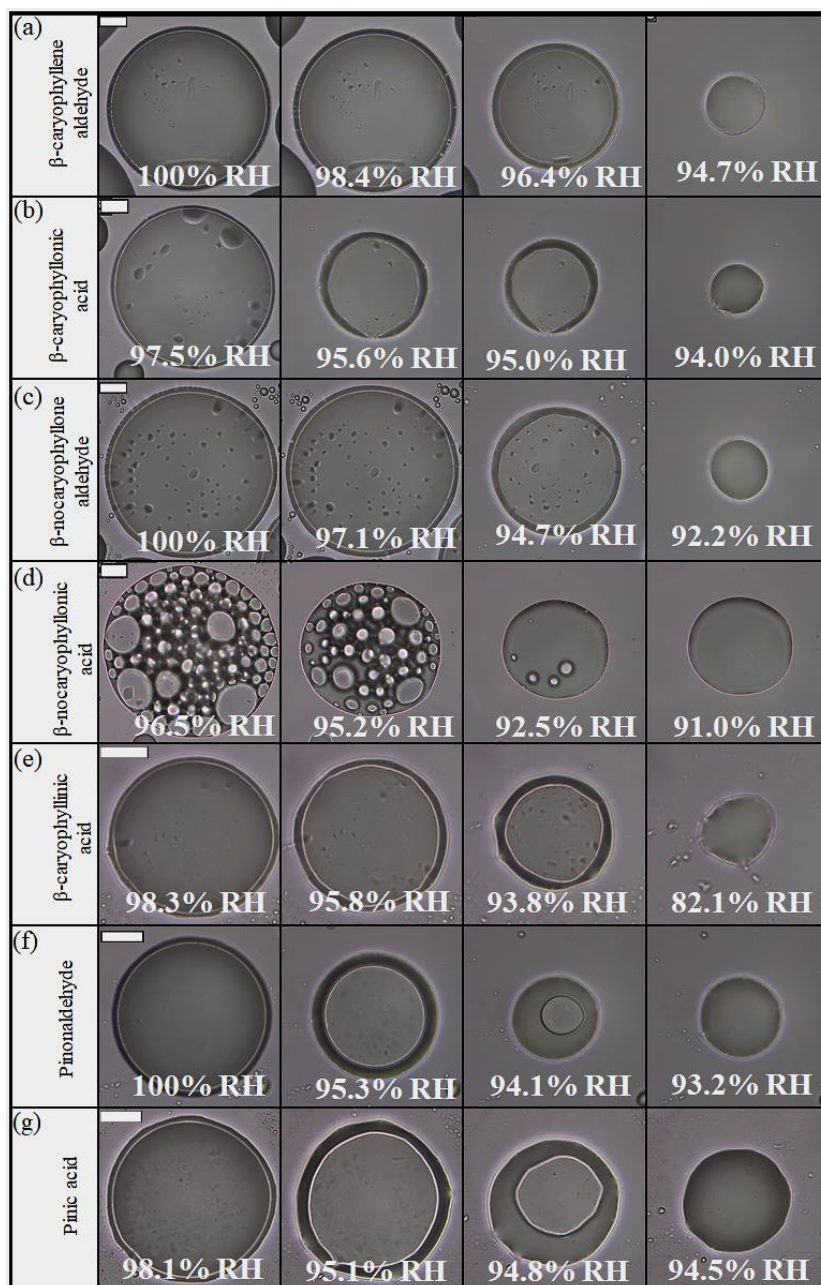
Figure 1. Optical images of particles for decreasing RH: (a) β-caryophyllene aldehyde, (b) β-caryophyllonic acid, (c) β-nocaryophyllone aldehyde, (d) β-nocaryophyllonic acid, (e) β-nocaryophyllinic acid, (f) pinonaldehyde, and (g) pinic acid. The last columns indicate the lower RH boundary for LLPS (LLPS$_{lower}$) with decreasing RH. The scale bar is 20 µm.

275
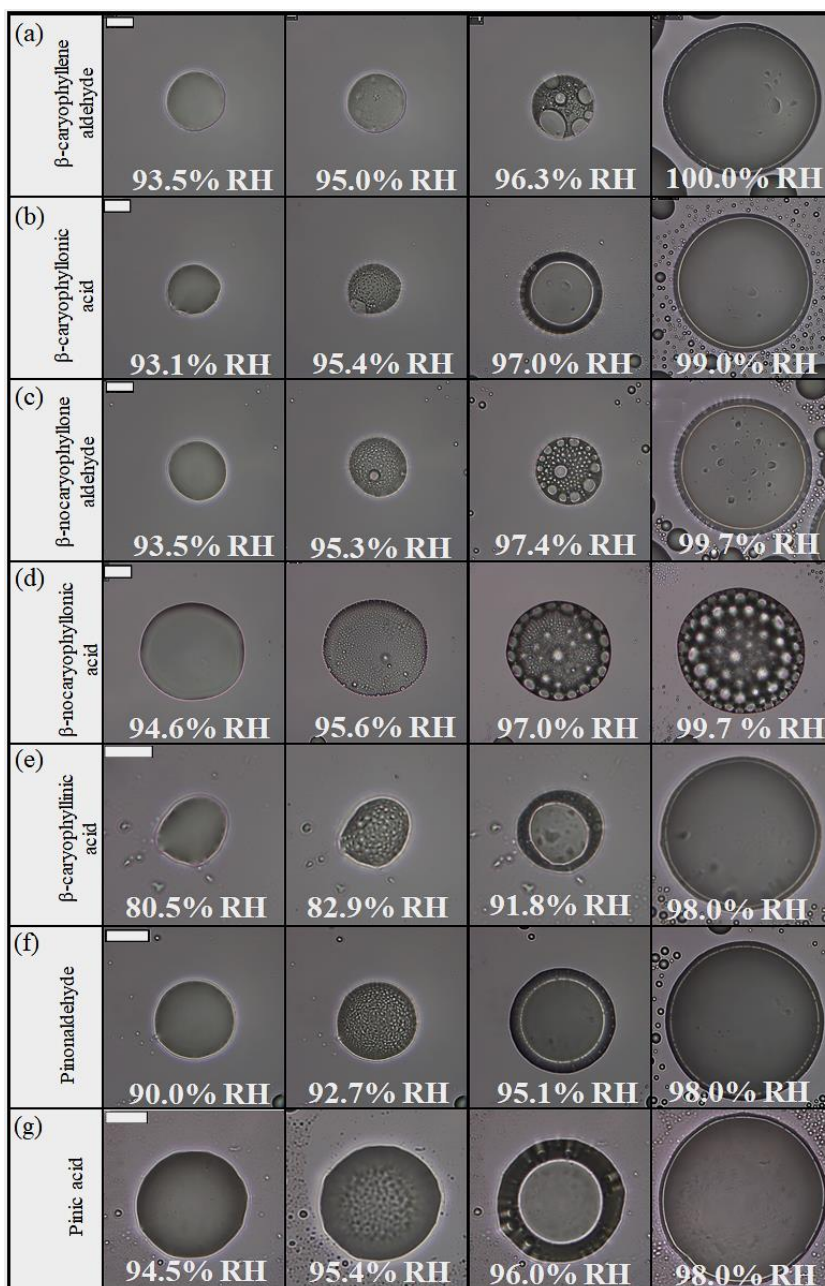
Figure 2. Optical images of particles for increasing RH: (a) β-caryophyllene aldehyde, (b) β-caryophyllonic acid, (c) β-nocaryophyllone aldehyde, (d) β-nocaryophyllonic acid, (e) β-nocaryophyllinic acid, (f) pinonaldehyde, and (g) pinic acid. The particles are the same ones in Fig. 1. The last columns indicate the upper RH boundary for LLPS (LLPS$_{upper}$) with increasing RH. The scale bar is 20 µm.
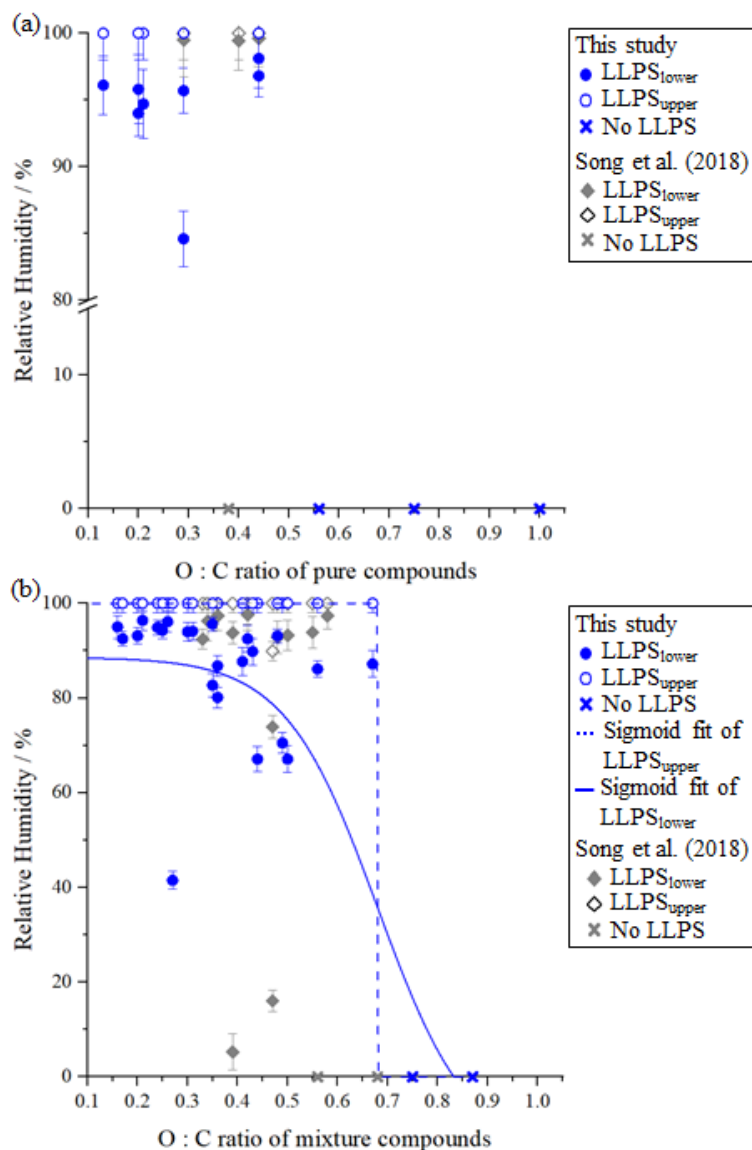
Figure 3. Relative humidity (RH) for LLPS as a function of the O:C of the organic particle consisting of: (a) one organic species, and (b) two organic species for increasing RH. Open blue circles are the LLPS upper boundary (LLPS$_{upper}$) with increasing RH, and closed blue circles are the LLPS lower boundary (LLPS$_{lower}$) with increasing RH. Each data point is included 4~5 particles within particle size ranges from 30 to 100 µm. The grey diamonds are the result from Song et al. (2018). Error bars represent 2σ of multiple measurements and the uncertainty from the RH calibration. The solid and dashed lines are Sigmoid-Boltzmann fits to all the data of LLPS$_{lower}$ and LLPS$_{upper}$.

290
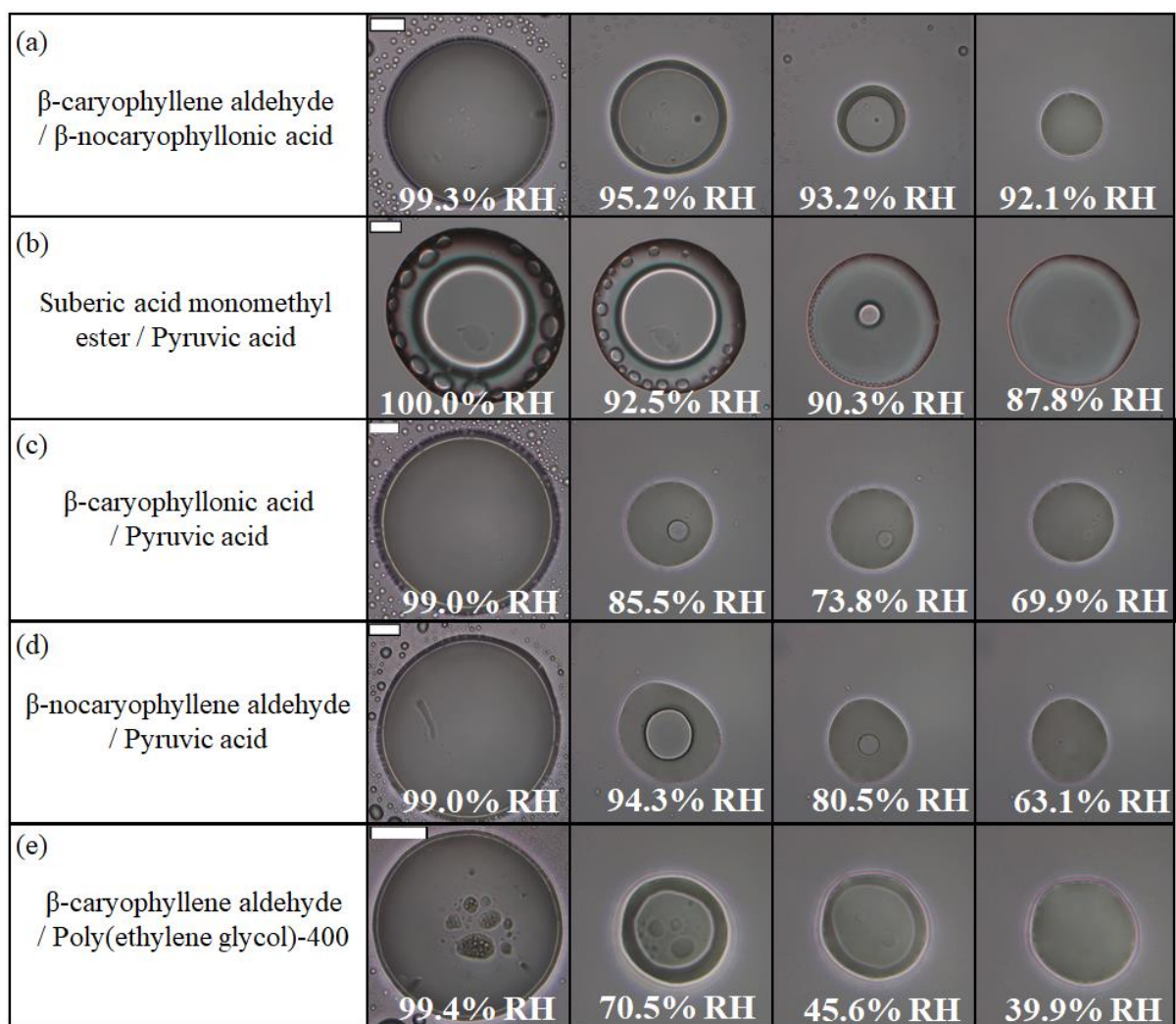
Figure 4. Optical images of two-component particles for decreasing RH: (a) β-caryophyllene aldehyde/β-nocaryophyllonic acid, (b) Suberic acid monomethyl ester/pyruvic acid, (c) β-caryophyllonic acid/pyruvic acid, (d) β-nocaryophyllene aldehyde/pyruvic acid, and (e) β-caryophyllene aldehyde/polyethylene glycol-400. The last columns indicate the lower RH boundary for LLPS (LLPS$_{lower}$) with decreasing RH. The scale bar is 20 µm.

295
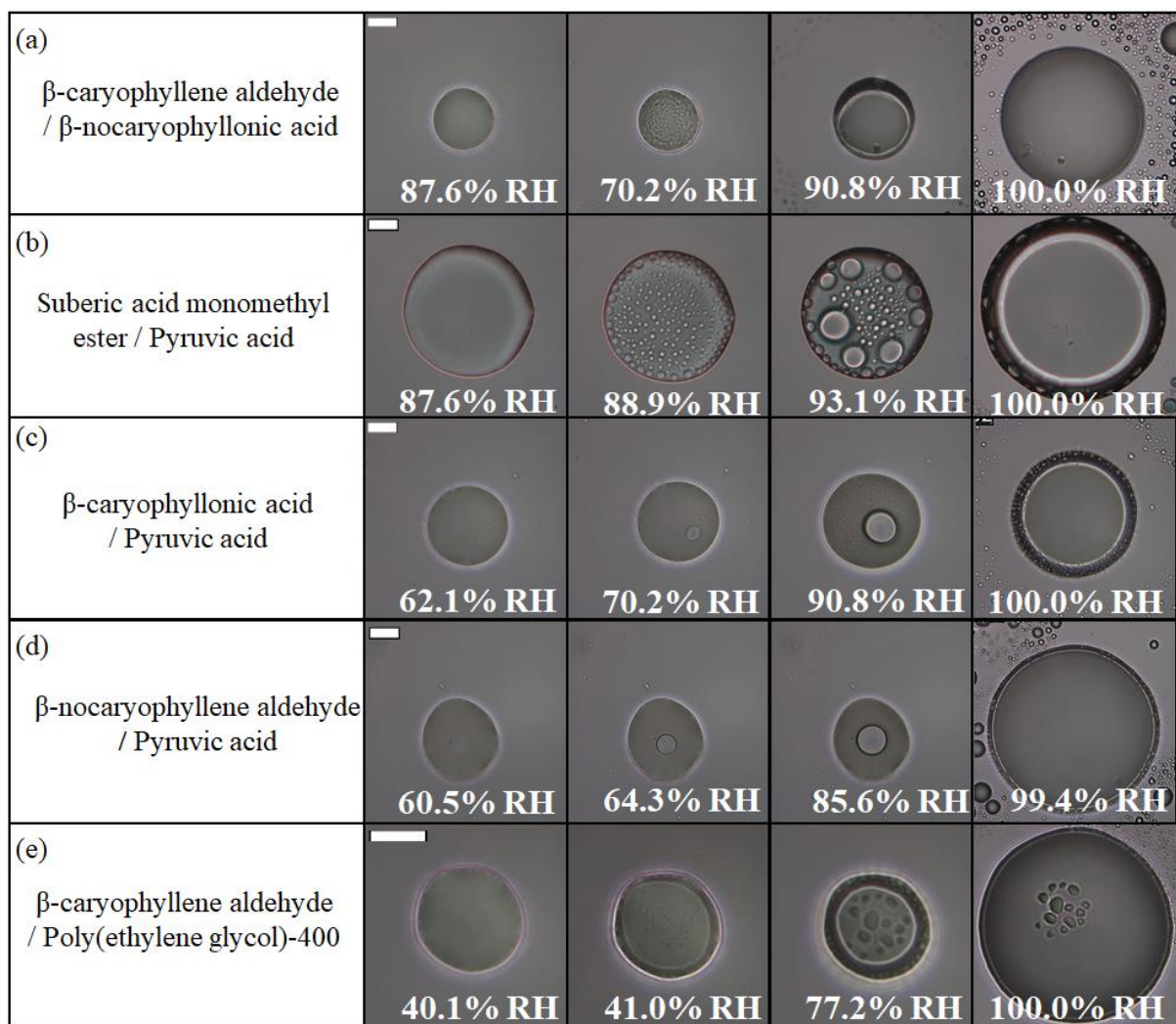
Figure 5. Optical images of two-component particles for increasing RH: (a) β-caryophyllene aldehyde/β-nocaryophyllonic acid, (b) Suberic acid monomethyl ester/pyruvic acid, (c) β-caryophyllonic acid/pyruvic acid, (d) β-nocaryophyllene aldehyde/pyruvic acid, and (e) β-caryophyllene aldehyde/polyethylene glycol-400. The particles are the same ones in Fig. 5. The last columns indicate the upper RH boundary for LLPS (LLPS$_{upper}$) with increasing RH. The scale bar is 20 µm.

Reference

Altaf, M. B., Zuend, A. and Freedman, M. A.: Role of nucleation mechanism on the size dependent morphology of organic aerosol, Chem. Commun., 52(59), 9220–9223, doi:10.1039/c6cc03826c, 2016.

Altaf, M. B. and Freedman, M. A.: Effect of Drying Rate on Aerosol Particle Morphology, J. Phys. Chem. Lett., 8(15), 3613–3618, doi:10.1021/acs.jpclett.7b01327, 2017.

Anttila, T., Kiendler-Scharr, A., Tillmann, R., and Mentel, T. F.: On the reactive uptake of gaseous compounds by organic-coated aqueous aerosols: Theoretical analysis and application to the heterogeneous hydrolysis of N_2O_5, J. Phys. Chem. A., 110, 10435– 10443, doi:10.1021/Jp062403c, 2006.

Bé, A. G., Upshur, M. A., Liu, P., Martin, S. T., Geiger, F. M. and Thomson, R. J.: Cloud activation potentials for atmospheric α-pinene and β-caryophyllene ozonolysis products, ACS Cent. Sci., 3(7), 715–725, doi:10.1021/acscentsci.7b00112, 2017.

Bertram, A. K., Martin, S. T., Hanna, S. J., Smith, M. L., Bodsworth, A., Chen, Q., Kuwata, M., Liu, A., You, Y. and Zorn, S. R.: Predicting the relative humidities of liquid-liquid phase separation, efflorescence, and deliquescence of mixed particles of ammonium sulfate, organic material, and water using the organic-to-sulfate mass ratio of the particle and the oxygen-to-carbon ele, Atmos. Chem. Phys., 11, 10995–11006, doi:10.5194/acp-11-10995-2011, 2011.

Brunamonti, S., Krieger, U. K., Marcolli, C. and Peter, T.: Redistribution of black carbon in aerosol particles undergoing liquid-liquid phase separation, Geophys. Res. Lett., 42(7), 2532–2539, doi:10.1002/2014GL062908, 2015.

Ciobanu, V. G., Marcolli, C., Krieger, U. K., Weers, U. and Peter, T.: Liquid-liquid phase separation in mixed organic/inorganic aerosol particles, J. Phys. Chem. A, 113(41), 10966–10978, doi:10.1021/jp905054d, 2009.

Cosman, L. M. and Bertram, A. K.: Reactive uptake of N_2O_5 on aqueous H_2SO_4 solutions coated with 1-component and 2-component monolayers, J. Phys. Chem. A., 112, 4625–4635, doi:10.1021/Jp8005469, 2008.

Cosman, L. M., Knopf, D. A. and Bertram, A. K.: N_2O_5 reactive uptake on aqueous sulfuric acid solutions coated with branched and straight-chain insoluble organic surfactants, J. Phys. Chem. A, 112(11), 2386–2396, doi:10.1021/jp710685r, 2008.

Donahue, N. M., Epstein, S. A., Pandis, S. N. and Robinson, A. L.: A two-dimensional volatility basis set: 1. Organic-aerosol mixing thermodynamics, Atmos. Chem. Phys., 11(7), 3303–3318, doi:10.5194/acp-11-3303-2011, 2011.

Fard, M. M., Krieger, U. K. and Peter, T.: Shortwave radiative impact of liquid-liquid phase separation in brown carbon aerosols, Atmos. Chem. Phys., 18, 13511–13530, doi:10.5194/acp-18-13511-2018, 2018.

Folkers, M., Mentel, T. F., and Wahner, A.: Influence of an organic coating on the reactivity of aqueous aerosols probed by the het- erogeneous hydrolysis of N_2O_5, Geophys. Res. Lett., 30, 1644, doi:10.1029/2003gl017168, 2003.

Freedman, M. A.: Phase separation in organic aerosol, Chem. Soc. Rev., 46, 7694–7705, doi:10.1039/C6CS00783J, 2017.

Gorkowski, K., Preston, T. C. and Zuend, A.: RH-humidity-dependent organic aerosol thermodynamics via an efficient reduced-complexity model, Atmos. Chem. Phys.,19, 13383-13407, doi:10.5194/acp-2019-495, 2019.

Guenther, A.: A global model of natural volatile organic compound emissions, J. Geophys. Res., doi:10.1029/94JD02950, 1995.

Hallquist, M., Wenger, J. C., Baltensperger, U., Rudich, Y., Simpson, D., Claeys, M., Dommen, J., Donahue, N. M., George, C., Goldstein, a. H., Hamilton, J. F., Herrmann, H., Hoffmann, T., Iinuma, Y., Jang, M., Jenkin, M. E., Jimenez, J. L., Kiendler-Scharr, a., Maenhaut, W., McFiggans, G., Mentel, T. F., Monod, a., Prévôt, a. S. H., Seinfeld, J. H., Surratt, J. D., Szmigielski, R. and Wildt, J.: The formation, properties and impact of secondary organic aerosol: current and emerging issues, Atmos. Chem. Phys., 9(14), 5155–5236, doi:10.5194/acp-9-5155-2009, 2009.

Ham, S., Babar, Z. Bin, Lee, J., Lim, H. and Song, M.: Liquid-liquid phase separation in secondary organic aerosol particles produced from α-pinene ozonolysis and α-pinene photo-oxidation with/without ammonia, Atmos. Chem. Phys., 19(14), 9321–9331, doi:10.5194/acp-2019-19, 2019.

Hänel, G.: The single-scattering albedo of atmospheric aerosol particles as a function of relative humidity, J. Atmos. Sci., 33(6), 1120–1124, doi:10.1175/1520-0469(1976)033<1120:tssaoa>2.0.co;2, 1976.

Heald, C. L., Ridley, D. A., Kreidenweis, S. M. and Drury, E. E.: Satellite observations cap the atmospheric organic aerosol budget, Geophys. Res. Lett., 37(24), 1–5, doi:10.1029/2010GL045095, 2010.

Henrot, A. J., Stanelle, T., Schröder, S., Siegenthaler, C., Taraborrelli, D. and Schultz, M. G.: Implementation of the MEGAN (v2.1) biogenic emission model in the ECHAM6-HAMMOZ chemistry climate model, Geosci. Model Dev., doi:10.5194/gmd-10-903-2017, 2017.

Hodas, N., Zuend, A., Schilling, K., Berkemeier, T., Shiraiwa, M., Flagan, R. C. and Seinfeld, J. H.: Discontinuities in hygroscopic growth below and above water saturation for laboratory surrogates of oligomers in organic atmospheric aerosols, Atmos. Chem. Phys., 16, 12767–12792, doi:10.5194/acp-16-12767-2016, 2016.

Jasper, J. J.: The surface tension of pure liquid compounds, J. Phys. And Chem. Ref. Data, vol 1, 841-1009, Doi: http://dx.doi.org/10.1063/1.3253106, 1972.

Jimenez, J. L., Canagaratna, M. R., Donahue, N. M., Prevot, a. S. H., Zhang, Q., Kroll, J. H., DeCarlo, P. F., Allan, J. D., Coe, H., Ng, N. L., Aiken, a. C., Docherty, K. S., Ulbrich, I. M., Grieshop, A. P., Robinson, a. L., Duplissy, J., Smith, J. D., Wilson, K. R., Lanz, V. a., Hueglin, C., Sun, Y. L., Tian, J., Laaksonen, A., Raatikainen, T., Rautiainen, J., Vaattovaara, P., Ehn, M., Kulmala, M., Tomlinson, J. M., Collins, D. R., Cubison, M. J., Dunlea, J., Huffman, J. A., Onasch, T. B., Alfarra, M. R., Williams, P. I., Bower, K., Kondo, Y., Schneider, J., Drewnick, F., Borrmann, S., Weimer, S., Demerjian, K., Salcedo, D., Cottrell, L., Griffin, R., Takami, a., Miyoshi, T., Hatakeyama, S., Shimono, A., Sun, J. Y., Zhang, Y. M., Dzepina, K., Kimmel, J. R., Sueper, D., Jayne, J. T., Herndon, S. C., Trimborn, a. M., Williams, L. R., Wood, E. C., Middlebrook, A. M., Kolb, C. E., Baltensperger, U., Worsnop, D. R., Dunlea, E. J., Huffman, J. A., Onasch, T. B., Alfarra, M. R., Williams, P. I., Bower, K., Kondo, Y., Schneider, J., Drewnick, F., Borrmann, S., Weimer, S., Demerjian, K., Salcedo, D., Cottrell, L., Griffin, R., Takami, a., Miyoshi, T., Hatakeyama, S., Shimono, A., Sun, J. Y., Zhang, Y. M., Dzepina, K., Kimmel, J. R., Sueper, D., Jayne, J. T., Herndon, S. C., Trimborn, a. M., Williams, L. R., Wood, E. C., Middlebrook, A. M., Kolb, C. E., Baltensperger, U., Worsnop, D. R., Dunlea, J., Huffman, J. A., et al.: Evolution of organic aerosols in the atmosphere, Science (80), 326(5959), 1525–1529, doi:10.1126/science.1180353, 2009.

Juranyi, Z., Gysel, M., Duplissy, J., Weingartner, E., Tritscher, T., Dommen, J., Henning, S., Ziese, M., Kiselev, A., Stratmann, F., George, I., and Baltensperger, U.: Influence of gas-to-particle partitioning on the hygroscopic and droplet activation behaviour of alpha-pinene secondary organic aerosol, Phys. Chem. Chem. Phys., 11, 8091–8097, https://doi.org/10.1039/B904162a, 2009.

Kanakidou, M., Seinfeld, J. H., Pandis, S. N., Barnes, I., Dentener, F. J., Facchini, M. C., Van Dingenen, R., Ervens, B., Nenes, A., Nielsen, C. J., Swietlicki, E., Putaud, J. P., Balkanski, Y., Fuzzi, S., Horth, J., Moortgat, G. K., Winterhalter, R., Myhre, C. E. L., Tsigaridis, K., Vignati, E., Stephanou, E. G. and Wilson, J.: Organic aerosol and global climate modelling: a review, Atmos. Chem. Phys., 5(4), 1053–1123, doi:10.5194/acp-5-1053-2005, 2005.

Krieger, U. K., Marcolli, C. and Reid, J. P.: Exploring the complexity of aerosol particle properties and processes using single particle techniques., Chem. Soc. Rev., 41(19), 6631–6662, doi:10.1039/c2cs35082c, 2012.

Kroll, J. H., Donahue, N. M., Jimenez, J. L., Kessler, S. H., Canagaratna, M. R., Wilson, K. R., Altieri, K. E., Mazzoleni, L. R., Wozniak, A. S., Bluhm, H., Mysak, E. R., Smith, J. D., Kolb, C. E. and Worsnop, D. R.: Carbon oxidation state as a metric for describing the chemistry of atmospheric organic aerosol., Nat. Chem., 3(2), 133–139, doi:10.1038/nchem.948, 2011.

Kwamena, N. O. A., Buajarern, J., and Reid, J. P.: Equilibrium morphology of mixed organic/inorganic/aqueous aerosol droplets: Investigating the effect of relative humidity and surfactants, J. Phys. Chem. A., 114, 5787–5795, doi:10.1021/Jp1003648, 2010.

Liu, P., Song, M., Zhao, T., Gunthe, S. S., Ham, S., He, Y., Qin, Y. M., Gong, Z., Amorim, J. C., Bertram, A. K. and Martin, S. T.: Resolving the mechanisms of hygroscopic growth and cloud condensation nuclei activity for organic particulate matter, Nat. Commun., doi:10.1038/s41467-018-06622-2, 2018.

Lam, H. K., Shum, S. M., Davies, J. F., Song, M., Zuend, A. and Chan, M. N.: Effects of Inorganic Salts on the Heterogeneous OH Oxidation of Organic Compounds: Insights from Methylglutaric Acid-Ammonium Sulfate, Atmos. Chem. Phys., 19, 9581-9593, 2019.

Marcolli, C. and Krieger, U. K.: Phase changes during hygroscopic cycles of mixed organic/inorganic model systems of tropospheric aerosols, J. Phys. Chem. A, 110(5), 1881–1893, doi:10.1021/jp0556759, 2006.

Martin, S. T.: Phase transitions of aqueous atmospheric particles, Chem. Rev., 100(9), 3403–3453, doi:10.1021/cr990034t, 2000.

415 McNeill, V. F., Yatavelli, R. L. N., Thornton, J. A., Stipe, C. B. and Landgrebe, O.: Heterogeneous OH oxidation of palmitic acid in single component and internally mixed aerosol particles: Vaporization and the role of particle phase, Atmos. Chem. Phys., 8(17), 5465–5476, doi:10.5194/acp-8-5465-2008, 2008.

Ng, N. L., Canagaratna, M. R., Zhang, Q., Jimenez, J. L., Tian, J., Ulbrich, I. M., Kroll, J. H., Docherty, K. S., Chhabra, P. S., Bahreini, R., Murphy, S. M., Seinfeld, J. H., Hildebrandt, L., Donahue, N. M.,

420 Decarlo, P. F., Lanz, V. A., Prévôt, A. S. H., Dinar, E., Rudich, Y. and Worsnop, D. R.: Organic aerosol components observed in northern hemispheric datasets from aerosol mass spectrometry, Atmos. Chem. Phys., 10(10), 4625–4641, doi:10.5194/acp-10-4625-2010, 2010.

Nozière, B., Kalberer, M., Claeys, M., Allan, J., D'Anna, B., Decesari, S., Finessi, E., Glasius, M., Grgić, I., Hamilton, J. F., Hoffmann, T., Iinuma, Y., Jaoui, M., Kahnt, A., Kampf, C. J., Kourtchev, I., Maenhaut,

425 W., Marsden, N., Saarikoski, S., Schnelle-Kreis, J., Surratt, J. D., Szidat, S., Szmigielski, R. and Wisthaler, A.: The molecular identification of organic compounds in the atmosphere: state of the art and challenges, Chem. Rev., 115(10), 3919–3983, doi:10.1021/cr5003485, 2015.

Obrien, R. E., Wang, B., Kelly, S. T., Lundt, N., You, Y., Bertram, A. K., Leone, S. R., Laskin, A. and Gilles, M. K.: Liquid-liquid phase separation in aerosol particles: Imaging at the nanometer scale, Environ.

430 Sci. Technol., 49(8), 4995–5002, doi:10.1021/acs.est.5b00062, 2015.

Olson, N. E., Lei, Z., Craig, R. L., Zhang, Y., Chen, Y., Lambe, A. T., Zhang, Z., Gold, A., Surratt, J. D. and Ault, A. P.: Reactive Uptake of Isoprene Epoxydiols Increases the Viscosity of the Core of Phase-Separated Aerosol Particles, ACS Earth Sp. Chem., 3(8), 1402–1414, doi:10.1021/acsearthspacechem.9b00138, 2019.

435 Ovadnevaite, J., Zuend, A., Laaksonen, A., Sanchez, K. J., Roberts, G., Ceburnis, D., Decesari, S., Rinaldi, M., Hodas, N., Facchini, M. C., Seinfeld, J. H. and O' Dowd, C.: Surface tension prevails over solute effect in organic-influenced cloud droplet activation, Nature, 546(7660), 637–641, doi:10.1038/nature22806, 2017.

Pankow, J. F.: Gas/particle partitioning of neutral and ionizing compounds to single and multi-phase

440 aerosol particles. 1. Unified modeling framework, Atmos. Environ., 37(24), 3323–3333, doi:10.1016/S1352-2310(03)00346-7, 2003.

Pant, A., Parsons, M. T. and Bertram, A. K.: Crystallization of aqueous ammonium sulfate particles internally mixed with soot and kaolinite: crystallization relative humidities and nucleation rates, J. Phys. Chem. A, 110(28), 8701–8709, doi:10.1021/jp060985s, 2006.

445 Papon, P.; Leblond, J.; Meijer, P. H. E. The Physics of Phase Transitions: Concepts and Applications, Springer, 1999.

Parsons, M. T., Mak, J., Lipetz, S. R. and Bertram, A. K.: Deliquescence of malonic, succinic, glutaric, and adipic acid particles, J. Geophys. Res. D Atmos., 109(6), 1–8, doi:10.1029/2003JD004075, 2004.

Petters, M. D., Kreidenweis, S. M., Snider, J. R., Koehler, K. A., Wang, Q., Prenni, A. J. and Demott, P.

450 J.: Cloud droplet activation of polymerized organic aerosol, Tellus, Ser. B Chem. Phys. Meteorol., 58(3), 196–205, doi:10.1111/j.1600-0889.2006.00181.x, 2006.

Petters, M. D., Kreidenweis, S. M., Snider, J. R., Koehler, K. A., Wang, Q., Prenni, A. J. and Demott, P. J.: Cloud droplet activation of polymerized organic aerosol, Tellus B, 58, 196–205, doi:10.1111/j.1600-0889.2006.00181.x, 2006.

455 Pöschl, U. and Shiraiwa, M.: Multiphase chemistry at the atmosphere–biosphere interface influencing climate and public health in the anthropocene, Chem. Rev., 115(10), 4440–4475, doi:10.1021/cr500487s, 2015.

Rastak, N., Pajunoja, A., Acosta Navarro, J. C., Ma, J., Song, M., Partridge, D. G., Kirkevåg, A., Leong, Y., Hu, W. W., Taylor, N. F., Lambe, A., Cerully, K., Bougiatioti, A., Liu, P., Krejci, R., Petäjä, T.,

460 Percival, C., Davidovits, P., Worsnop, D. R., Ekman, A. M. L., Nenes, A., Martin, S., Jimenez, J. L., Collins, D. R., Topping, D. O., Bertram, A. K., Zuend, A., Virtanen, A. and Riipinen, I.: Microphysical explanation of the RH-dependent water affinity of biogenic organic aerosol and its importance for climate, Geophys. Res. Lett., 44(10), 5167–5177, doi:10.1002/2017GL073056, 2017.

Reid, J. P., Dennis-Smither, B. J., Kwamena, N.-O. A., Miles, R. E. H., Hanford, K. L., and Homer, C.

465 J.: The morphology of aerosol particles consisting of hydrophobic and hydrophilic phases: hydrocarbons, alcohols and fatty acids as the hydropho- bic component, Phys. Chem. Chem. Phys., 13, 15559–15572, doi:10.1039/C1CP21510H,doi:10.1039/C1CP21510H, 2011.

Renbaum-Wolff, L., Song, M., Marcolli, C., Zhang, Y., Liu, P. F., Grayson, J. W., Geiger, F. M., Martin, S. T. and Bertram, A. K.: Observations and implications of liquid-liquid phase separation at high relative

470   humidities in secondary organic material produced by α-pinene ozonolysis without inorganic salts, Atmos. Chem. Phys., 16(12), 7969–7979, doi:10.5194/acp-16-7969-2016, 2016.

Riva, M., Chen, Y., Zhang, Y., Lei, Z., Olson, N. E., Boyer, H. C., Narayan, S., Yee, L. D., Green, H. S., Cui, T., Zhang, Z., Baumann, K., Fort, M., Edgerton, E., Budisulistiorini, S. H., Rose, C. A., Ribeiro, I. O., Oliveira, R. L. E., Dos Santos, E. O., Machado, C. M. D., Szopa, S., Zhao, Y., Alves, E. G., De Sá, S.

475   S., Hu, W., Knipping, E. M., Shaw, S. L., Duvoisin Junior, S., De Souza, R. A. F., Palm, B. B., Jimenez, J. L., Glasius, M., Goldstein, A. H., Pye, H. O. T., Gold, A., Turpin, B. J., Vizuete, W., Martin, S. T., Thornton, J. A., Dutcher, C. S., Ault, A. P. and Surratt, J. D.: Increasing Isoprene Epoxydiol-to-Inorganic Sulfate Aerosol Ratio Results in Extensive Conversion of Inorganic Sulfate to Organosulfur Forms: Implications for Aerosol Physicochemical Properties, Environ. Sci. Technol., 53(15), 8682–8694,

480   doi:10.1021/acs.est.9b01019, 2019.

Sanchez, K. J., Roberts, G. C., Calmer, R., Nicoll, K., Hashimshoni, E., Rosenfeld, D., Ovadnevaite, J., Preissler, J., Ceburnis, D., O'Dowd, C. and Russell, L. M.: Top-down and bottom-up aerosol-cloud-closure: towards understanding sources of uncertainty in deriving cloud radiative flux, Atmos. Chem. Phys., 17, 9797–9814, doi:doi.org/10.5194/acp-17-9797-2017, 2017.

485   Sakulyanontvittaya, T., Duhl, T., Wiedinmyer, C., Helmig, D., Matsunaga, S., Potosnak, M., Milford, J. and Guenther, A.: Monoterpene and sesquiterpene emission estimates for the United States, Environ. Sci. Technol., 42(5), 1623–1629, doi:10.1021/es702274e, 2008.

Schill, G. P. and Tolbert, M. A.: Heterogeneous ice nucleation on phase-separated organic-sulfate particles: effect of liquid vs. glassy coatings, Atmos. Chem. Phys., 13(9), 4681–4695, doi:10.5194/acp-

490   13-4681-2013, 2013.

Seaton, A., MacNee, W., Donaldson, K. and Godden, D.: Particulate air pollution and acute health effects., Lancet, 345(8943), 176–178, doi:10.1016/S0140-6736(95)90173-6, 1995.

Shelby, J. E. Introduction to Glass Science and Technology; The Royal Society of Chemistry: Cambridge, U.K., 1995

495   Shiraiwa, M., Zuend, A. A., Bertram, A. K. and Seinfeld, J. H.: Gas-particle partitioning of atmospheric aerosols: interplay of physical state, non-ideal mixing and morphology., Phys. Chem. Chem. Phys., 15, 11441–11453, doi:10.1039/c3cp51595h, 2013.

Shiraiwa, M., Ueda, K., Pozzer, A., Lammel, G., Kampf, C. J., Fushimi, A., Enami, S., Arangio, A. M., Fröhlich-Nowoisky, J., Fujitani, Y., Furuyama, A., Lakey, P. S. J., Lelieveld, J., Lucas, K., Morino, Y., Pöschl, U., Takahama, S., Takami, A., Tong, H., Weber, B., Yoshino, A. and Sato, K.: Aerosol health effects from molecular to global scales, Environ. Sci. Technol., 51, 13545–13567, doi:10.1021/acs.est.7b04417, 2017.

Song, M., Marcolli, C., Krieger, U. K., Zuend, A. and Peter, T.: Liquid-liquid phase separation and morphology of internally mixed dicarboxylic acids/ammonium sulfate/water particles, Atmos. Chem. Phys., 12, 2691–2712, doi:10.5194/acp-12-2691-2012, 2012a.

Song, M., Marcolli, C., Krieger, U. K., Zuend, A. and Peter, T.: Liquid-liquid phase separation in aerosol particles: Dependence on O:C, organic functionalities, and compositional complexity, Geophys. Res. Lett., 39, L19801, doi:10.1029/2012GL052807, 2012b.

Song, M. J., Marcolli, C., Krieger, U. K., Lienhard, D. M., and Pe- ter, T.: Morphologies of mixed organic/inorganic/aqueous aerosol droplets, Faraday Discuss., 165, 289–316, https://doi.10.1039/C3fd00049d, 2013

Song, M., Liu, P., Martin, S. T. and Bertram, A. K.: Liquid-liquid phase separation in particles containing secondary organic material free of inorganic salts, Atmos. Chem. Phys., 17, 11261–11271, doi:10.5194/acp-17-11261-2017, 2017.

Song, M., Ham, S., Andrews, R. J., You, Y. and Bertram, A. K.: Liquid-liquid phase separation in organic particles containing one and two organic species: importance of the average O:C, Atmos. Chem. Phys., doi:10.5194/acp-18-12075-2018, 2018.

Veghte, D. P., Bittner, D. R. and Freedman, M. A.: Cryo-transmission electron microscopy imaging of the morphology of submicrometer aerosol containing organic acids and ammonium sulfate, Anal. Chem., 86(5), 2436–2442, doi:10.1021/ac403279f, 2014.

Winston, P. W. and Bates, D. H.: Saturated solutions for the control of humidity in biological research, Ecology, 41(1), 232–237, 1960.

Xiaohong, L. and Jian, W.: How important is organic aerosol hygroscopicity to aerosol indirect forcing?, Environ. Res. Lett., 5(4), 44010, doi:10.1088/1748-9326/5/4/044010, 2010.

You, Y., Renbaum-Wolff, L. and Bertram, A. K.: Liquid-liquid phase separation in particles containing organics mixed with ammonium sulfate, ammonium bisulfate, ammonium nitrate or sodium chloride, Atmos. Chem. Phys., 13, 11723–11734, doi:10.5194/acp-13-11723-2013, 2013.

You, Y., Smith, M. L., Song, M., Martin, S. T. and Bertram, A. K.: Liquid-liquid phase separation in atmospherically relevant particles consisting of organic species and inorganic salts, Int. Rev. Phys. Chem., 33(1), 43–77, doi:10.1080/0144235X.2014.890786, 2014.

Zhang, Y., Chen, Y., Lambe, A. T., Olson, N. E., Lei, Z., Craig, R. L., Zhang, Z., Gold, A., Onasch, T. B., Jayne, J. T., Worsnop, D. R., Gaston, C. J., Thornton, J. A., Vizuete, W., Ault, A. P. and Surratt, J. D.: Effect of the Aerosol-Phase State on Secondary Organic Aerosol Formation from the Reactive Uptake of Isoprene-Derived Epoxydiols (IEPOX), Environ. Sci. Technol. Lett., 5(3), 167–174, doi:10.1021/acs.estlett.8b00044, 2018.

Zhang, Y., Chen, Y., Lei, Z., Olson, N. E., Riva, M., Koss, A. R., Zhang, Z., Gold, A., Jayne, J. T., Worsnop, D. R., Onasch, T. B., Kroll, J. H., Turpin, B. J., Ault, A. P. and Surratt, J. D.: Joint Impacts of Acidity and Viscosity on the Formation of Secondary Organic Aerosol from Isoprene Epoxydiols (IEPOX) in Phase Separated Particles, ACS Earth Sp. Chem., 3(12), 2646–2658, doi:10.1021/acsearthspacechem.9b00209, 2019.

Zhang, Q., Jimenez, J. L., Canagaratna, M. R., Allan, J. D., Coe, H., Ulbrich, I., Alfarra, M. R., Takami, A., Middlebrook, A. M., Sun, Y. L., Dzepina, K., Dunlea, E., Docherty, K., DeCarlo, P. F., Salcedo, D., Onasch, T., Jayne, J. T., Miyoshi, T., Shimono, A., Hatakeyama, S., Takegawa, N., Kondo, Y., Schneider, J., Drewnick, F., Borrmann, S., Weimer, S., Demerjian, K., Williams, P., Bower, K., Bahreini, R., Cottrell, L., Griffin, R. J., Rautiainen, J., Sun, J. Y., Zhang, Y. M. and Worsnop, D. R.: Ubiquity and dominance of oxygenated species in organic aerosols in anthropogenically-influenced Northern Hemisphere midlatitudes, Geophys. Res. Lett., 34(13), 1–6, doi:10.1029/2007GL029979, 2007.Zuend, A. and Seinfeld, J. H.: Modeling the gas-particle partitioning of secondary organic aerosol: The importance of liquid-liquid phase separation, Atmos. Chem. Phys., 12, 3857–3882, doi:10.5194/acp-12-3857-2012, 2012.

Zuend, A., Marcolli, C., Peter, T. and Seinfeld, J. H.: Computation of liquid-liquid equilibria and phase stabilities: Implications for RH-dependent gas/particle partitioning of organic-inorganic aerosols, Atmos. Chem. Phys., 10(16), 7795–7820, doi:10.5194/acp-10-7795-2010, 2010.